Polyhedron 222 (2022) 115914

Contents lists available at ScienceDirect

Polyhedron

journal homepage: www.elsevier.com/locate/poly

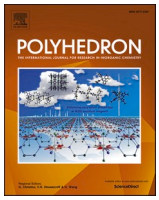

Evaluation of the interaction of nanojars with biomolecules found in human body fluids

Wisam A. Al Isawi, Mia L. Jawor, Christian K. Hartman, Gellert Mezei [1,*]

Department of Chemistry, Western Michigan University, Kalamazoo, MI 49008, USA

A B S T R A C T

In this work, the stability of nanojars of the formula $[CO_3\subset\{Cu(OH)(Rpz)\}_n]^{2-}$ (pz = pyrazole derivative; R = H, 4-($CH_3OCH_2CH_2O$) or 4-($CH_3(OCH_2CH_2)_3O$); n = 27, 29, 31) in the presence of biological molecules found in human body fluids was investigated using electrospray ionization mass spectrometry (with small biomolecules) and UV–vis spectroscopy (with proteins and serum). Lipids (triglycerides and cholesterol), glucose, urea, uric acid, creatine, creatinine, amino acids (glycine, alanine, glutamic acid, tyrosine), bilirubin, adenine, ascorbic acid, albumin, γ-globulins and fibrinogen display varying degrees of reactivity towards nanojars, ranging from no interaction to substitution of nanojars by pyrazolate ligand replacement to complete nanojar breakdown. Nanojars appear to be overall stable in pure human serum solutions (pH 8.0).

1. Introduction

Nanojars constitute a unique class of coordination complexes with the general formula $[anion\subset\{Cu(OH)(Rpz)\}_n]^{2-}$ (Rpz– = pyrazolate or derivative, with R in the 4- and/or 3/5-position of the pz ring; R = H, aliphatic or aromatic hydrocarbons, oligoethers, alcohols, halogens; n = 26–36; anion = sulfate, carbonate, hydrogen phosphate, etc.), which have recently been developed into robust anion-binding and extracting agents [1–14]. Formed by self-assembly from the constituent moieties (Cu^{2+}, HO^- and pz^- ions), nanojars consist of stacks of three or four $\{Cu(OH)(pz)\}_x$ (x = 6–14, except 11) metallacycles held together around the central incarcerated anion by a multitude of weak Cu–O interactions and hydrogen bonds (Fig. 1). The binding between the metallacycles and the anion is surprisingly strong. Indeed, an aqueous solution of Ba^{2+} ions is unable to precipitate the highly insoluble barium salt of the incarcerated anion (such as $BaSO_4$ in the case of sulfate) when stirred together with a solution of nanojars [2,3,12]. The robustness of nanojars suggests that they might also be used for the extraction and transport of copper ions. As demonstrated earlier, no other metals than copper are able to form nanojars [10]. Moreover, the possibility of using nanojars in therapeutic applications, such as the treatment of copper-related diseases, became an intriguing prospect.

Copper is an essential element for living organisms, including humans. As copper takes part in all aspects of metabolism in different parts of the body, efficient transport of copper is critical for the proper functioning of living organisms [15]. Deficiencies in copper transport, caused by mutations in transport proteins, lead to serious diseases, and either copper deficiency (Menkes disease [16]) or excess copper (Wilson's disease [17]) is observed in certain organs within the body [18]. Thus far, there is no cure for Menkes disease, which typically begins during infancy and most affected newborns die within the first few years of life. Wilson's disease is also fatal when left untreated; current medical treatments cause painful side effects or complications, and occasionally a liver transplant is required. It is evident that new forms of treatment are needed for curing these lethal diseases. Nanojars might be able to deliver copper and treat Menkes disease where other copper-containing drugs fail, or they might be vehicles for removing copper from the body in the case of Wilson's disease. Another potential use of nanojars is as vehicles for the targeted transport of anticancer drugs to tumors, where the local acidity would lead to breakdown of nanojars and release of the cargo. The pH of normal tissues is slightly basic in the range of 7.2–7.5, whereas tumor cells are known to be mildly acidic in the range of 6.4–7.0 [19].

Pyrazole derivatives are found in natural products [20] and are often used in pharmaceuticals [21]. For example, 3-nonylpyrazole, the first pyrazole-containing natural product derivative obtained in 1954, has a strong antibiotic activity [22]. 4-Methylpyrazole (fomepizole) is an effective antidote used in treating methanol and ethylene glycol poisoning [23], and it is listed on the World Health Organization's List of Essential Medicines. Other common pyrazole-based drugs include celecoxib and sildenafil.

Body fluids, which could distribute nanojars throughout the body

* Corresponding author.
E-mail address: gellert.mezei@wmich.edu (G. Mezei).

[1] Dedicated to Professor Ionel Haiduc on the occasion of his 85th birthday.

https://doi.org/10.1016/j.poly.2022.115914
Received 15 March 2022; Accepted 13 May 2022
Available online 18 May 2022
0277-5387/© 2022 Elsevier Ltd. All rights reserved.

(blood, lymph and intracellular/interstitial fluids) or excrete nanojars from the body (urine), are complex mixtures containing various macromolecules (proteins), as well as small organic molecules (metabolites and nutrients) and inorganic ions (electrolytes). We have demonstrated earlier that nanojars are stable to electrolytes (mineral salts, including various alkali and alkaline-earth metal ions, such as Na^+, K^+ and Ca^{2+}, as well as anions, such as chloride, carbonate, sulfate and phosphate).[5] The aim of the current work is to test the possible interaction of nanojars with major organic metabolites (urea, uric acid, bile pigments, creatinine), nutrients (carbohydrates, amino acids, lipids, creatine, adenine, cholesterol, ascorbic acid) and human plasma proteins (albumin, γ-globulins and fibrinogen) found in body fluids (Fig. 2), using electrospray ionization mass spectrometry in negative ion mode (ESI-MS(–)) and UV–vis spectroscopy. Also, the solution stability of nanojars in human serum is investigated.

2. Results and discussion

Analysis of the interaction of nanojars with biological molecules was performed either by mass spectrometry (in the case of small molecules), or UV–vis spectroscopy (in the case of proteins). ESI-MS was not suitable for the analysis of proteins as they do not ionize well without additives, and commonly used additives that improve ionization efficiency (such as organic acids or their ammonium salts) lead to the breakdown of nanojars. Also, the water soluble nanojar derivative $Na_2[CO_3\subset\{Cu(OH)(TEGpz)\}_n]$ (TEG = 4-($CH_3(OCH_2CH_2)_3O$); n = 27, 29, 31), which would be used with aqueous protein solutions, has poor ionization efficiency. Nanojars can only be analyzed by ESI-MS in the negative mode as dianions; only the counterion (such as Bu_4N^+ at *m/z* 242) and no nanojar peaks are observed by ESI-MS(+). When synthesized, $[CO_3\subset\{Cu(OH)(Rpz)\}_n]^{2-}$ nanojars form in a mixture consisting of species with n = 27, 29, 30 and 31. The ratio of these species can vary slightly from batch to batch. In this work, one mole of nanojar refers to $[CO_3\subset\{Cu(OH)(pz)\}_{29}]^{2-}$, which represents the average amount of nanojars observed in the as-synthesized nanojar mixtures employed.

2.1. Analysis by ESI-MS

For the ESI-MS(–) experiments, solutions of nanojars with increasing amounts (molar equivalents, per mole of nanojar as defined above) of the biological molecules were employed. In the case of glucose, cholesterol, urea, bilirubin, amino acids and ascorbic acid, the experiments were performed using the parent nanojar, $(Bu_4N)_2[CO_3\subset\{Cu(OH)(pz)\}_n]$ (n = 27, 29, 30, 31) in acetonitrile or butyronitrile (cholesterol and triglycerides) or dimethylformamide (bilirubin). Peaks of the nanojars are observed at *m/z* 2023 (n = 27), *m/z* 2171 (n = 29), *m/z* 2245 (n = 30; small amount) and *m/z* 2318 (n = 31). Adenine, uric acid, creatinine and creatine are poorly soluble in organic solvents; therefore, experiments based on these molecules were performed in a 2:1 mixture of water and acetonitrile. Because the parent nanojars are not soluble in the H_2O:CH_3CN (2:1) mixture, the ethyleneglycol derivative, $Na_2[CO_3\subset\{Cu(OH)(MEGpz)\}_n]$ (MEG = 4-($CH_3OCH_2CH_2O$); n = 27, 29, 31) was used instead. A major nanojar peak is observed at *m/z* 3023 (n = 27), and minor peaks at *m/z* 3245 (n = 29) and *m/z* 3466 (n = 31). It should be noted that smaller fragments (such as Cu_1–Cu_6 breakdown products) are expected to have higher ionization efficiency than nanojars, due to their higher charge-to-mass ratio. Therefore, the relative intensities of nanojar vs. breakdown product peaks in the ESI-MS spectra do not reflect actual ratios in the sample. Furthermore, the samples are getting diluted as increasing amounts of the biomolecule solutions are added to the nanojar solution, leading to diminishing of the nanojar signal intensity at increasing equivalents of biomolecules added.

2.1.1. Triglycerides and cholesterol

Nanojars are stable in the presence of triglycerides and cholesterol, and no nanojar substitution occurs. Only traces of low-nuclearity Cu-complexes (*m/z* 542, $[Cu_3O(pz)_5]^-$; *m/z* 673, $[Cu_4O(pz)_6]^-$; *m/z* 852, $[(Bu_4N)Cu_3O(pz)_6]^-$) are observed with 100 equiv of cholesterol (Fig. S1), whereas in the case of triglycerides no low-nuclearity Cu-species are detected even with 100 equiv of triglycerides (Fig. 3). Because at high equivalents of the added biomolecule the nanojar solution is significantly diluted, the intensity of the nanojar peaks decreases and small amounts of contaminants at low *m/z* values become more noticeable.

2.1.2. Glucose

Nanojars are stable in the presence of glucose ($C_6H_{12}O_6$), as no breakdown products are observed even at 200 equiv of glucose (Figs. S2 and S3). However, the nanojar size distribution does change with increasing equivalents of glucose. In particular, the peak corresponding to the Cu_{31} nanojar gradually diminishes and new peaks at *m/z* 2104 and 2372, corresponding to hitherto unidentified nanojar species appear. Above 5 equiv of glucose, the peak corresponding to the Cu_{29} nanojar gradually gains intensity and becomes the dominant peak above 60 equiv of glucose.

2.1.3. Urea, uric acid, creatine and creatinine

No low-nuclearity Cu-species are detected and no nanojar substitution is observed (Figs. S4–S10). However, small amounts of a blue precipitate are found in solutions containing more than 10 equiv of creatinine.

2.1.4. Adenine

In the presence of 1–4 equiv of adenine, nanojars exchange up to

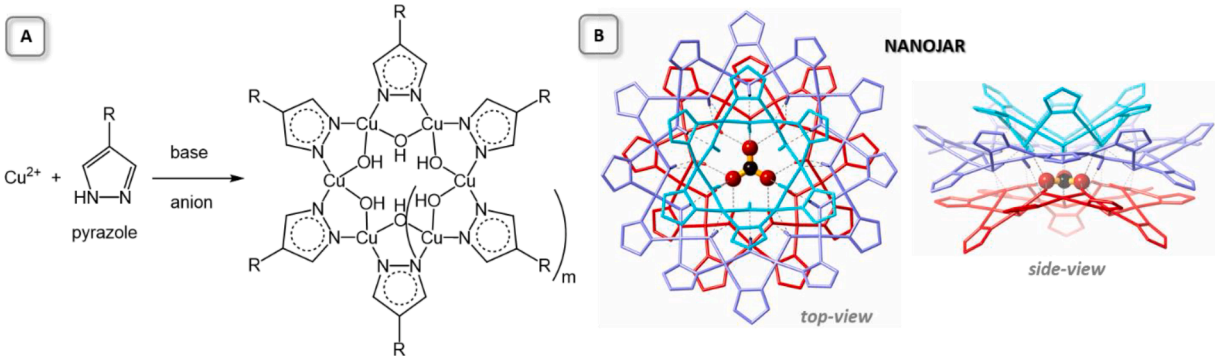

Fig. 1. A) Formation of the $[Cu(OH)(Rpz)]_x$ rings in nanojars (x = 6 – 14, except 11; m = 1 – 9; R = H, aliphatic or aromatic hydrocarbons, oligoethers, halogens). B) Crystal structure of the carbonate-incarcerating nanojar, $[CO_3\subset\{Cu(OH)(Hpz)\}_{27}]^{2-}$ (x = 6, 12, 9). Pentagons denote pyrazolates (cyan: $[Cu(OH)(pz)]_6$, m = 1; purple: $[Cu(OH)(pz)]_{12}$, m = 7; red: $[Cu(OH)(pz)]_9$, m = 4). ((Colour online.))

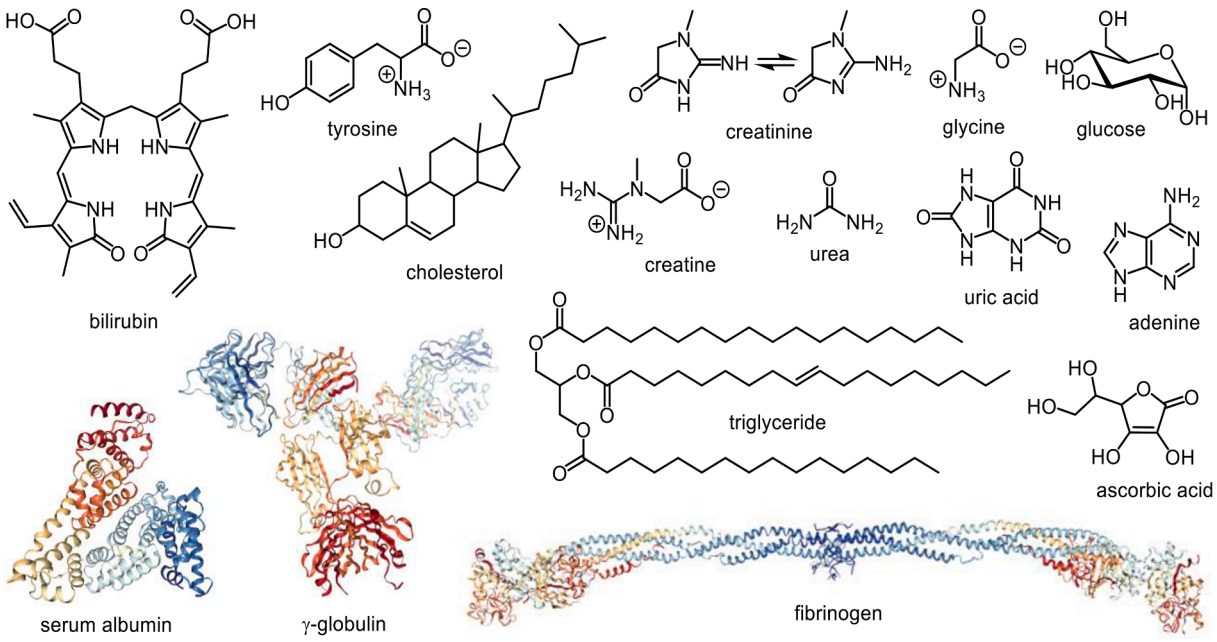

Fig. 2. Examples of common proteins, amino acids, sugars, lipids, nucleobases, bile pigments (bilins), metabolites and nutrients found in body fluids. Protein figures were drawn using crystal structures from the Protein Data Bank.

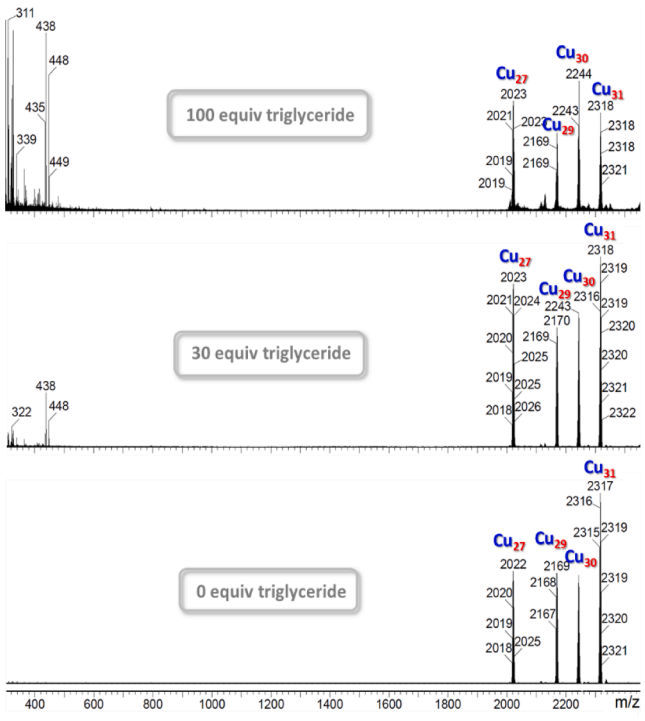

Fig. 3. ESI-MS(–) spectra of $[CO_3\subset\{Cu(OH)(pz)\}_n]^{2-}$ (n = 27, 29, 30, 31) nanojars in butyronitrile with increasing amounts of added triglyceride.

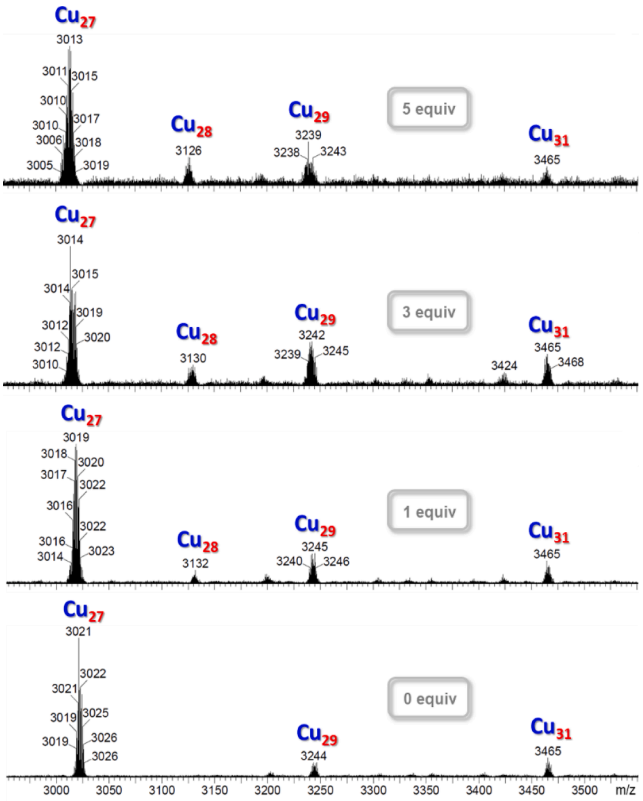

Fig. 4. ESI-MS(–) spectra of $[CO_3\subset\{Cu(OH)(MEGpz)\}_n]^{2-}$ (n = 27, 28, 29, 31) nanojars in CH_3CN/H_2O with increasing amounts of added adenine.

four pyrazolate ($MEGpz^-$) units with adeninate (ade; $C_5H_4N_5^-$), as indicated by the formation of substituted nanojars $[CO_3\subset\{Cu_n(OH)_n(MEGpz)_{n-y}(ade)_y\}]^{2-}$ (y = 1–4; n = 27, *m/z* 3019–3009; n = 28, *m/z* 3130–3120; n = 29, *m/z* 3241–3231; n = 31, *m/z* 3463–3452) (Fig. 4). The formation of adenine adducts, $[CO_3\subset\{Cu(OH)(MEGpz)\}_n(ade)\}]^{2-}$ (n = 28, *m/z* 3201; n = 30, *m/z* 3423; n = 32, *m/z* 3645) is also observed (Figs. S11 and S12). In samples prepared with 5 or more equiv of adenine per nanojar there is more nanojar decomposition, as indicated by increasing amounts of small copper-adeninate fragments, such as $[Cu(ade)_2]^-$ (*m/z* 332), $[Cu_2(ade)_3]^-$ (*m/z* 529), $[Cu_2(ade)_4]^-$ (*m/z* 664), $[Cu_2(OH)(ade)_4]^-$ (*m/z* 681), $[Cu_2(OH)(H_2O)(ade)_4]^-$ (*m/z* 699) and $[Cu_2(ade)_5]^-$ (*m/z* 798). Adeninate is known to form discrete mononuclear [24], dinuclear (paddlewheel) [25] and polynuclear [26] complexes, as well as metal–organic frameworks [27] with copper.

2.1.5. Bilirubin

With 1 equiv of bilirubin ($C_{33}H_{36}N_4O_6$) added, nanojar degradation products show up along with intact, nonsubstituted nanojars (Fig. S13). Breakdown products include $[Cu(C_{33}H_{32}N_4O_6)]^{2-}$ (*m/z* 322), $[Cu(C_{33}H_{33}N_4O_6)]^{-}$ (*m/z* 645) and $[CuO(C_{33}H_{36}N_4O_6)]^{-}$ (*m/z* 664), as well as dehydro-derivatives (biliverdin) $[Cu(C_{33}H_{30}N_4O_6)]^{-}$ (*m/z* 642) and $[(Bu_4N)Cu(C_{33}H_{30}N_4O_6)]^{-}$ (*m/z* 885), decarboxylated derivatives $[Cu(C_{32}H_{30}N_4O_4)]^{2-}$ (*m/z* 598) and $[Cu(C_{32}H_{30}N_4O_4)]^{2-}$ (*m/z* 554), and dehydrated derivative $[Cu(C_{32}H_{28}N_4O_3)]^{2-}$ (*m/z* 580). The Cu_{27} nanojar appears to be the most sensitive as it is not detected above 3 equiv. of bilirubin. Other nanojars also break down gradually and only degradation products are observed above 10 equiv of bilirubin (Fig. S14).

2.1.6. Amino acids

With increasing equivalents of added amino acids, nanojars gradually break down and give rise to low-nuclearity copper complexes. No nanojar substitution is observed. In the case of glycine (gly = $C_2H_4NO_2^-$), breakdown products include $[Cu(gly)_2]^-$ (*m/z* 212), $[Cu(gly)_3]^-$ (*m/z* 286), $[Cu_2(pz)(gly)_2]^-$ (*m/z* 342), $[Cu_2(gly)_3]^-$ (*m/z* 349), $[Cu_2(gly)_3(C_2H_3NO_2)]^-$ (*m/z* 422), $[Cu_2(OH)(pz)(gly)_3]^-$ (*m/z* 433), $[Cu_2(pz)_2(gly)_3]^-$ (*m/z* 483) and $[Cu_2(pz)(gly)_4]^-$ (*m/z* 490) (Fig. S15). Sodium glycinate, however, does not react with nanojars; only peaks corresponding to intact nanojars are observed in a solution with 60 equiv of sodium glycinate after standing for 3 days. With alanine (ala = $C_3H_6NO_2^-$), breakdown products including $[Cu_2(pz)(ala)_2]^-$ (*m/z* 370), $[Cu_2(ala)_3]^-$ (*m/z* 391), $[Cu_2(ala)_4]^-$ (*m/z* 479), $[Cu_3(OH)(pz)_6]^-$ (*m/z* 610), $[Cu_3(OH)(pz)_5(ala)]^-$ (*m/z* 631), $[Cu_3(OH)(pz)_4(ala)_2]^-$ (*m/z* 652), $[Cu_3(OH)(pz)_3(ala)_3]^-$ (*m/z* 673), $[Cu_3(OH)(pz)_2(ala)_4]^-$ (*m/z* 694) and $[Cu_3(OH)(pz)(ala)_5]^-$ (*m/z* 715) are observed above 10 equiv of alanine (Fig. S16). With glutamic acid (glu = $C_5H_7NO_4^{2-}$) breakdown products include $[Cu(glu)]^-$ (*m/z* 209), $[Cu_2(pz)(glu)]^-$ (*m/z* 339), $[(Na)Cu(glu)_2]^-$ (*m/z* 377), $[Cu_2(pz)(glu)_2]^-$ (*m/z* 484), $[(Bu_4N)Cu(glu)_2]^-$ (*m/z* 596), $[Cu_2O_2(gluH)_4]^-$ (*m/z* 744) and $[Cu_2(pz)(glu)_2(gluH)_2]^-$ (*m/z* 777) above 10 equiv of glutamic acid (Fig. S17). Similar behavior is observed with tyrosine as well (Figs. S18 and S19).

2.1.7. Ascorbic acid

In the presence of nanojars, ascorbic acid (vitamin C) is found to be oxidized to 2,3,4,5-tetrahydroxypentanoic acid ($C_5H_{10}O_6$), as indicated by the formation of substituted nanojars $[CO_3\subset\{Cu_{29}(\mu\text{-}OH)_{29}(\mu\text{-}pz)_{28}(C_5H_9O_6)\}]$ (n = 29, *m/z* 2220; n = 31, *m/z* 2367) (Fig. 5). With increasing amounts of ascorbic acid, a gradual breakdown of the nanojars is observed and hexanuclear (*m/z* 1227; assigned to $Cu_6O_2(pz)_6(C_5H_9O_6)_2(CH_3CN)_2$ based on similar species observed earlier) along with smaller nuclearity fragments become prevalent.[6,9] With increasing equivalents of ascorbic acid the color of the solution gradually lightens and changes to green–blue, and above 7 equiv precipitation occurs.

2.2. Analysis by UV–vis spectroscopy

For studies involving proteins in aqueous solutions and blood serum, a nanojar with good water solubility was needed. The parent pz-nanojars are not soluble in water, and the MEGpz-derivatives are poorly soluble in water. Therefore, the triethyleneglycol derivatives $Na_2[CO_3\subset\{Cu(OH)(TEGpz)\}_n]$ (TEG = 4-$(CH_3(OCH_2CH_2)_3O)$; n = 27, 29, 31) were employed for the UV–vis experiments.

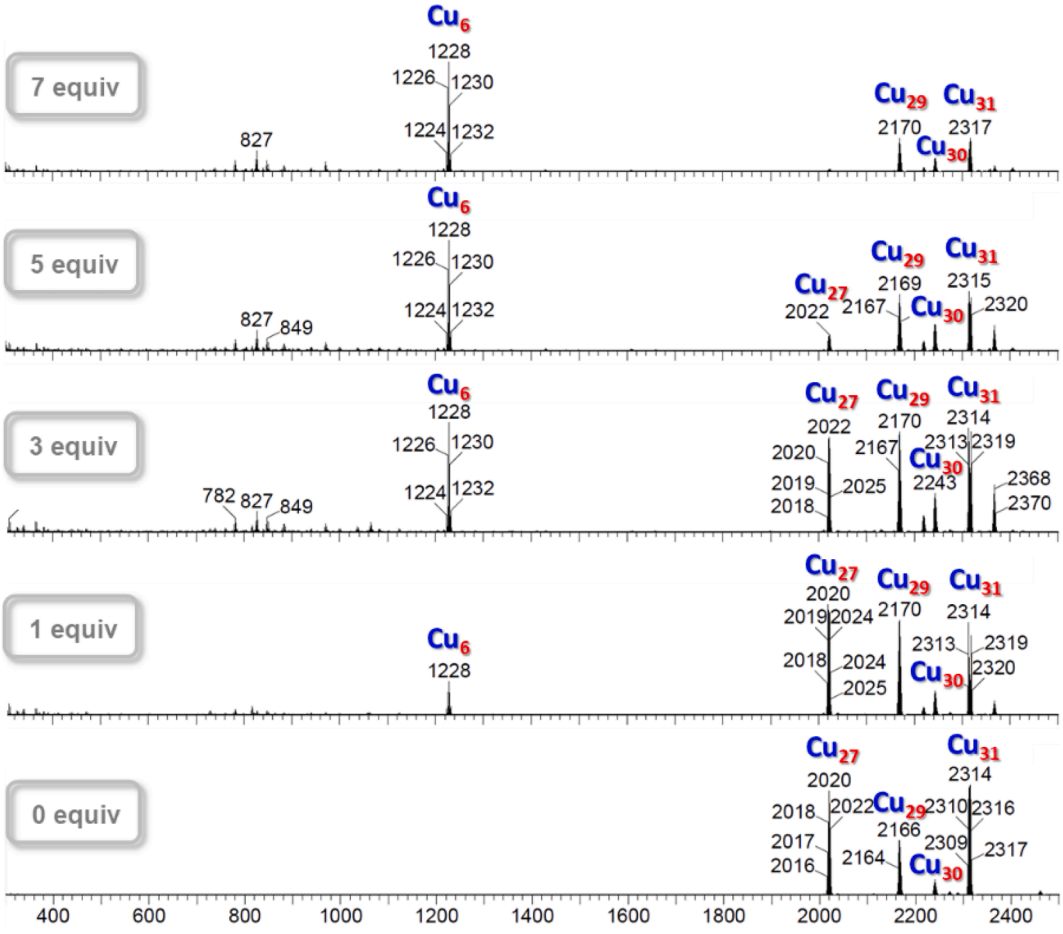

Fig. 5. ESI-MS(–) spectra of $[CO_3\subset\{Cu(OH)(pz)\}_n]^{2-}$ (n = 27, 29, 30, 31) nanojars in CH_3CN with increasing amounts of ascorbic acid.

2.2.1. Albumin, γ-globulins and fibrinogen

As seen in Fig. 6, nanojars display absorption maxima at λ_{max} 343 and 607 nm corresponding to charge-transfer and *d-d* transitions, respectively. In the presence of added proteins, the UV–vis spectra show a slight decrease in the absorbance of the nanojars with albumin, and a more substantial decrease in the case of γ-globulins and fibrinogen. Also, a slight blue-shift of the signal at 600 nm is observed with γ-globulins and a more significant red-shift with fibrinogen.

2.2.2. Human serum

Fig. 7 shows comparisons of the absorption of nanojars at 607 nm in water vs serum, at different concentrations (6×10^{-4} M, 3×10^{-4} M and 6×10^{-5} M). In the serum sample employed (pH: 8.0; osmolality: 285 mosmol/kg; total proteins: 50 g/L; cholesterol: 1.16 g/L; triglycerides: 0.52 g/L; glucose: 1.04 g/L), the concentration of proteins is approximately 4×10^{-4} M for albumin, 1×10^{-4} M for γ-globulins and 1×10^{-5} M for fibrinogen (based on typical levels in the blood). Thus, the corresponding nanojar:protein molar ratios are approximately 1.5:1, 6:1 and 60:1 in the case of the 6×10^{-4} M nanojar solution, 0.75:1, 3:1 and 30:1 in the case of the 3×10^{-4} M nanojar solution, and 0.15:1, 0.6:1 and 6:1 in the case of the 6×10^{-5} M nanojar solution.

2.3. Discussion

Nanojar substitution was observed in the presence of adenine, which led to the replacement of up to 4 pyrazolate ligands by adeninate. At higher equivalents of adenine, low-nuclearity copper-adeninate fragments were also observed. Bilirubin, which possesses two carboxylic acid moieties, reacts with nanojars even at 1 equiv, leading to a significant fraction of mononuclear copper-bilirubinate fragments without nanojar substitution. The observed *m/z* values for these fragments indicate that bilirubin is quadruply deprotonated and copper is bound in its tetrapyrrole pocket derived from porphyrin. Above 10 equiv of bilirubin, nanojars break down and the ESI-MS(–) spectrum is dominated by copper-biliverdinate (dehydro-derivative of bilirubinate).

Similarly, amino acids lead to nanojar breakdown, forming mono-, di- and trinuclear copper complexes without nanojar substitution. This observation is in contrast to the behavior of aliphatic carboxylic acids, of which up to 10 equiv can be incorporated into nanojars in form of their conjugate bases replacing pyrazolate ligands,[9] and it is likely due to the neighboring amino group which leads to chelation along with the carboxylate moiety and disrupts the nanojar structure. In the absence of acidic protons, the conjugate base of amino acids does not replace pyrazolate ligands in nanojars, as indicated by the unchanged ESI-MS(–) spectrum of a solution of nanojars after adding 60 equiv of sodium glycinate. Again, this is contrary to the observed reactivity of aliphatic carboxylates with nanojars.[9] It should be noted that many biomolecules, including amino acids and bilirubin, are not free when circulating in blood, but they are found attached to serum albumin.

In the presence of ascorbic acid, nanojar species substituted by 2,3,4,5-tetrahydroxypentanoate (an oxidation product of ascorbic acid) are detected along with intact nanojars and a hexanuclear copper-pyrazolate/tetrahydroxypentanoate breakdown product. This result suggests that as opposed to α-amino acids, only the carboxylate moiety of the α-hydroxy acid is employed in binding to the copper centers in nanojars. Thus, the conjugate base of the α-hydroxy acid acts as bridging instead of chelating ligand, which is compatible with the nanojar structure. The presence of the lower nuclearity fragment is consistent with the acidity of ascorbic acid and its carboxylic acid oxidation product, which leads to partial protonation of the OH groups and breakdown of the nanojar.

In the case of pure albumin, γ-globulins and fibrinogen, the decrease in signal intensity at 607 nm and shift in the value of λ_{max} suggest some interaction between nanojars and proteins. In pure serum, however, the small decrease in signal intensity (6–8% for the 3–6 × 10–^{4} M nanojar solutions) compared to the pure aqueous solution indicates that

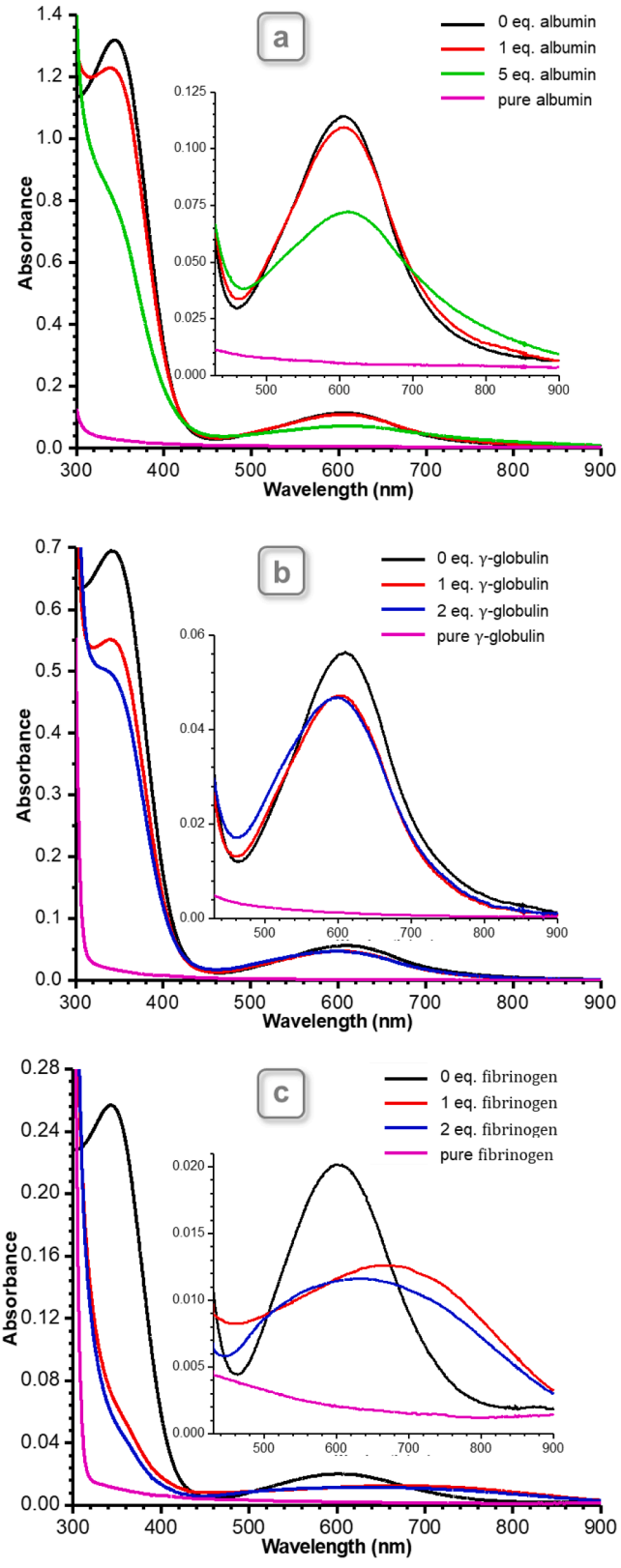

Fig. 6. UV–vis spectra of $[CO_3C\{Cu(OH)(TEGpz)\}_n]^{2-}$ nanojars in water with (a) serum albumin, (b) γ-globulins, and (c) fibrinogen. The spectra are corrected for dilution.

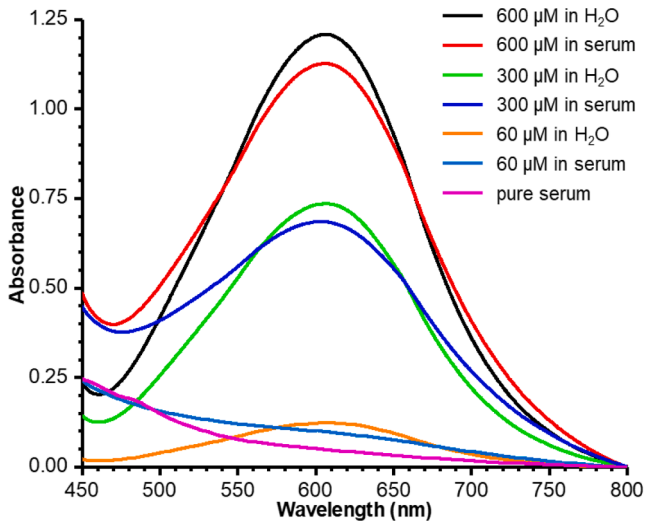

Fig. 7. UV–vis spectra of $CO_3\subset\{Cu(OH)(TEGpz)\}_n]^{2-}$ nanojars in water and serum at varying concentrations.

complete breakdown of the nanojars is implausible, as the extinction coefficient of possible breakdown products, such as trinuclear copper-pyrazolate complexes, is over 16-fold smaller (ε_{607nm} = 2.5 × 10^3 L mol^{-1} cm^{-1} for $Na_2[CO_3\subset\{Cu(OH)(TEGpz)\}_n]$; ε_{600nm} = 2.6 × 10^3 L mol^{-1} cm^{-1} for $(Bu_4N)_2[CO_3\subset\{Cu(OH)(pz)\}_n]$; ε_{630nm} = 0.16 × 10^3 L mol^{-1} cm^{-1} for $Cu_3(OH)(pz)_3(H_2O)(NO_3)_2$). Given that complete breakdown of nanojars would result in ~ 10 trinuclear units per nanojar, the corresponding decrease in absorption intensity is expected to be ~ 40%. Lower concentrations of nanojars are impractical for analysis by UV–vis spectroscopy, as serum is light brown-yellow in color and has significant absorption at 607 nm.

3. Conclusions

The interaction of nanojars with 17 representative biomolecules commonly found in human body fluids has been investigated using ESI-MS(–) spectrometry and UV–vis spectroscopy. ESI-MS(–) shows no low-nuclearity nanojar breakdown products in the presence of lipids (triglycerides and cholesterol), glucose, urea, uric acid, creatine and creatinine. Acidic compounds react with nanojars, resulting either in the replacement of the pyrazolate ligand with the conjugate base of the compound and maintaining the overall nanojar structure, or in breakdown of the nanojar to low-nuclearity (Cu_1–Cu_6) complexes.

Blood proteins (albumin, γ-globulins and fibrinogen) appear to interact with nanojars, suggested by a decrease in absorption intensity in the corresponding UV–vis spectra and blue- or red-shift in the case of γ-globulins and fibrinogen, respectively. It is possible that some nanojar sizes are more reactive than others, as suggested by the ESI-MS(–) studies using small biomolecules. Nevertheless, 3–6 × 10^{-4} M nanojar solutions in pure serum, which is a complex mixture of small biomolecules and proteins at slightly basic pH (8.0 in the case of the serum sample employed), display only a minor decrease in the signal intensity of visible absorption ruling out the complete breakdown of nanojars.

4. Experimental section

4.1. General methods

Human serum (cat. no. H5667), albumin from human serum (cat. no. A3782), γ-globulins from human blood (cat. no. G4386), fibrinogen type I from human plasma (cat. no. F3879) and bilirubin (mixed isomers, cat. no. B4126) were purchased from Sigma-Aldrich. Commercial soybean oil was used for triglycerides. All reagents and solvents are commercially available and are used as received (THF is inhibited with 250 ppm BHT). $(Bu_4N)_2[CO_3\subset\{Cu(\mu\text{-}OH)(\mu\text{-}pz)\}_n]$, $Na_2[CO_3\subset\{Cu(\mu\text{-}OH)(\mu\text{-}4\text{-}(CH_3OCH_2CH_2O)pz)\}_n]$ and $Na_2[CO_3\subset\{Cu(\mu\text{-}OH)(\mu\text{-}4\text{-}(CH_3(OCH_2CH_2)_3O)pz)\}_n]$ (n = 27–31) nanojars are prepared according to published procedures.[4,6] UV–vis spectra are collected on a Shimadzu UV-1650PC instrument.

4.2. Solution preparation for ESI-MS analysis

Solvents were LC-MS (acetonitrile and water) or Chromasolv Plus grade (dimethylformamide). Solutions with increasing amounts of molar equivalents of biomolecules were obtained by adding the required amounts of stock solutions of the biomolecules to a stock solution of nanojars. All solutions were left standing overnight and were filtered before analysis. Control samples of nanojar solutions, as well as solutions of nanojars in the presence of biological molecules are stable over time and do not show decomposition, as verified by ESI-MS and UV–vis measurements. It has also been shown by ESI-MS that nanojars are stable at high dilution (at least to 10^{-7} M).[9] For a given sample, the ratio between peaks of nanojars of different sizes as well as of nanojars and eventual breakdown products (in the presence of certain biological molecules) is constant to within ± 5% on duplicate runs in the ESI-MS spectra.

4.2.1. Cholesterol and triglycerides

A 1.0 × 10^{-4} M solution of nanojars was prepared by dissolving $(Bu_4N)_2[CO_3\subset\{Cu(OH)(pz)\}_n]$ (12.1 mg, 2.5 × 10^{-3} mmol, based on an average n = 29) in butyronitrile and diluting to volume in a 25 mL volumetric flask. A 5.0 × 10^{-3} M cholesterol stock solution is prepared by dissolving cholesterol (48.4 mg, 1.25 × 10^{-4} mmol) in butyronitrile and diluting to volume in a 25 mL volumetric flask. A 5.0 × 10^{-3} M triglyceride stock solution (using a MW of 885 g/mol, which corresponds to triolein) was prepared by dissolving soybean oil (44.3 mg, 48.2 μL, 5 × 10^{-5} mmol) in butyronitrile and diluting to volume in a 10 mL volumetric flask.

4.2.2. Glucose, amino acids, ascorbic acid and urea

A 1.0 × 10^{-4} M solution of nanojars was prepared by dissolving $(Bu_4N)_2[CO_3\subset\{Cu(OH)(pz)\}_n]$ (7.2 mg, 1.5 μmol, based on an average n = 29) in 15 mL of acetonitrile. A 5.0 × 10^{-3} M stock solution of glucose (poorly soluble in acetonitrile) was prepared in 10 mL of a 94:1 mixture of acetonitrile and water. 2.2 × 10^{-3} M stock solutions of amino acids were prepared in water, except for tyrosine (poorly soluble in water) which was prepared in a mixture of 5 mL of acetonitrile and 30 mL of water. 3.3 × 10^{-3} M stock solutions of urea and ascorbic acid were prepared in 25 mL of acetonitrile (with a trace of DMF added in the case of ascorbic acid).

4.2.3. Adenine, uric acid, creatine and creatinine

A 1.0 × 10^{-4} M solution of nanojars was prepared by dissolving $Na_2[CO_3\subset\{Cu(OH)(MEGpz)\}_n]$ (9.8 mg, 1.5 μmol, based on an average n = 29) in 15 mL of a 2:1 mixture of water and acetonitrile. Stock solutions of adenine, uric acid, creatinine and creatine (insoluble or poorly soluble in acetonitrile) were prepared at a concentration of 1.0 × 10^{-3} M in 25 mL of a 2:1 mixture of water and acetonitrile.

4.2.4. Bilirubin

A 2.5 × 10^{-5} M solution of nanojars was prepared by dissolving $(Bu_4N)_2[\{Cu(OH)(pz)\}_n]$ (3 mg, 6.25 × 10^{-4} mmol, based on an average n = 29) in dimethylformamide and diluting to volume in a 25 mL volumetric flask. A 2.5 × 10^{-4} M solution of bilirubin (not soluble in acetonitrile or a 1:1 acetonitrile-dimethylformamide mixture) was prepared by dissolving bilirubin (7.3 mg, 1.25 × 10^{-2} mmol) in dimethylformamide and diluting to volume in a 50 mL volumetric flask. Brown vials were used for the MS samples due to the light sensitivity of bilirubin.

4.3. Solution preparation for UV–vis analysis

For the experiments with albumin, the following solutions were prepared in water using $Na_2[CO_3\subset\{Cu(OH)(TEGpz)\}_n]$ (TEG-NJs, based on an average n = 29) and solid albumin: a) 5×10^{-5} M TEG-NJs, b) 5×10^{-5} M TEG-NJs + 5×10^{-5} M albumin, c) 5×10^{-5} M TEG-NJs + 2.5×10^{-4} M albumin, and d) 5×10^{-5} M albumin. For the γ-globulin experiments, aqueous solutions of 2.5×10^{-5} M TEG-NJs and 1.25×10^{-5} M γ-globulins were prepared. Solutions containing 1 and 2 molar equivalents of γ-globulins were obtained by adding 800 μL of the γ-globulin solution per equivalent to 4 mL of nanojar solution. For the fibrinogen experiments, aqueous solutions of 1×10^{-5} M TEG-NJs and 2.5×10^{-5} M fibrinogen solutions were prepared. Solutions containing 1 and 2 M equivalents of fibrinogen were obtained by adding 1 mL of fibrinogen solution per equivalent to 2.5 mL nanojar solution. For experiments with serum, 6×10^{-4} M, 3×10^{-4} M and 6×10^{-5} M solutions of TEG-NJs were prepared either in pure serum, or pure water. All solutions were filtered before analysis (small amounts of white solids were observed). Calculations are based on the following molecular weights: human serum albumin – 66,437 g/mol, γ-globulin – 160,000 g/mol, fibrinogen – 340,000 g/mol.

4.4. Determination of molar extinction coefficients for $(Bu_4N)_2[\{Cu(OH)(pz)\}_n]$, $Na_2[\{Cu(OH)(TEGpz)\}_n]$ and $Cu_3(OH)(pz)_3(H_2O)(NO_3)_2$

Solutions of $Na_2[CO_3\subset\{Cu(OH)(pz)\}_n]$ nanojars (using n = 29 for an average MW) at concentrations of 5.0–70 $\times 10^{-6}$ M and the trinuclear complex $Cu_3(OH)(pz)_3(H_2O)(NO_3)_2$ at concentrations of 1.0–5.0 $\times 10^{-4}$ M were prepared in tetrahydrofuran by serial dilution. With $Na_2[CO_3\subset\{Cu(OH)(TEGpz)\}_n]$ nanojars, solutions in water at concentrations of 3.0×10^{-5} M, 6.0×10^{-5} M and 3.0×10^{-4} M were used. Molar extinction coefficients were determined using UV–vis spectroscopy as shown in the supporting information file (Figs. S20–S22).

4.5. Mass spectrometry

Mass spectrometric analyses are performed on a Waters Synapt G1 HDMS instrument, using electrospray ionization (ESI). Sample solutions are infused by a syringe pump at 5–10 μL/min and nitrogen is supplied as nebulizing gas at 200 L/h. The electrospray capillary voltage is set to 2.5 kV, with a desolvation temperature of 110 °C. The sampling and extraction cones are maintained at 40 and 2.4 V, respectively, at 80 °C. All observed isotope patterns match the corresponding predicted ones (nanojar isotope patterns are detailed in reference 4). Some of the low-nuclearity breakdown products are fully or partially reduced species (Cu(II) is easily reduced to Cu(I) during ESI-MS(–) analysis) [28]. Occasionally, minor contamination due to detergent residues, such as $[C_{10}H_{21}C_6H_4SO_3]^-$ (*m/z* 297.2), $[C_{11}H_{23}C_6H_4SO_3]^-$ (*m/z* 311.2), $[C_{12}H_{25}C_6H_4SO_3]^-$ (*m/z* 325.2), $[C_{13}H_{27}C_6H_4SO_3]^-$ (*m/z* 339.2), or other unidentified contaminants (*e.g.*, *m/z* 233) is observed.

CRediT authorship contribution statement

Wisam A. Al Isawi: Investigation, Methodology, Formal analysis, Data curation, Validation, Visualization, Writing – review & editing. **Mia L. Jawor:** Investigation, Formal analysis, Visualization, Writing – review & editing. **Christian K. Hartman:** Investigation, Writing – review & editing. **Gellert Mezei:** Conceptualization, Funding acquisition, Project administration, Resources, Methodology, Supervision, Formal analysis, Data curation, Visualization, Writing – original draft, Writing – review & editing.

Declaration of Competing Interest

The authors declare that they have no known competing financial interests or personal relationships that could have appeared to influence the work reported in this paper.

Acknowledgements

This material is based on work supported by Western Michigan University (College of Arts and Sciences Discovery and Dissemination Award) and the National Science Foundation (Grant No. CHE-1808554).

Appendix A. Supplementary data

Supplementary data to this article can be found online at https://doi.org/10.1016/j.poly.2022.115914.

References

[1] G. Mezei, P. Baran, R.G. Raptis, Anion encapsulation by neutral supramolecular assemblies of cyclic Cu^{II} complexes: A series of five polymerization isomers, [{*cis*-Cu^{II}(μ-OH)(μ-pz)}$_n$], n = 6, 8, 9, 12, and 14, Angew. Chem. Int. Ed. 43 (2004) 574–577.
[2] I.R. Fernando, S.A. Surmann, A.A. Urech, A.M. Poulsen, G. Mezei, Selective total encapsulation of the sulfate anion by neutral nanojars, Chem. Commun. 48 (2012) 6860–6862.
[3] G. Mezei, Incarceration of one or two phosphate or arsenate species within nanojars, capped nanojars and nanohelicages: helical chirality from two closely-spaced, head-to-head PO_4^{3-} or AsO_4^{3-} ions, Chem. Commun. 51 (2015) 10341–10344.
[4] B.M. Ahmed, B.R. Szymczyna, S. Jianrattanasawat, S.A. Surmann, G. Mezei, Survival of the fittest nanojar: stepwise breakdown of polydisperse Cu_{27}–Cu_{31} nanojar mixtures into monodisperse $Cu_{27}(CO_3)$ and $Cu_{31}(SO_4)$ nanojars, Chem. Eur. J. 22 (2016) 5499–5503.
[5] B.M. Ahmed, G. Mezei, From ordinary to extraordinary: insights into the formation mechanism and pH-dependent assembly/disassembly of nanojars, Inorg. Chem. 55 (2016) 7717–7728.
[6] B.M. Ahmed, B. Calco, G. Mezei, Tuning the structure and solubility of nanojars by peripheral ligand substitution, leading to unprecedented liquid-liquid extraction of the carbonate ion from water into aliphatic solvents, Dalton Trans. 45 (20) (2016) 8327–8339.
[7] B.M. Ahmed, C.K. Hartman, G. Mezei, Sulfate-incarcerating nanojars: solution and solid-state studies, sulfate extraction from water, and anion exchange with carbonate, Inorg. Chem. 55 (2016) 10666–10679.
[8] a) B.M. Ahmed, G. Mezei, Accessing the inaccessible: discrete multinuclear coordination complexes and selective anion binding attainable only by tethering ligands together, Chem. Commun. 56 (2017) 1029–1032;
b) W.A. Al Isawi, A.Z. Salome, B.M. Ahmed, M. Zeller, G. Mezei, Selective binding of anions by rigidified nanojars: sulfate vs. carbonate, Org. Biomol. Chem. 19 (2021) 7641–7654.
[9] C.K. Hartman, G. Mezei, Mapping the intricate reactivity of nanojars toward molecules of varying acidity and their conjugate bases leading to exchange of pyrazolate ligands, Inorg. Chem. 56 (2017) 10609–10624.
[10] W.A. Al Isawi, B.M. Ahmed, C.K. Hartman, A.N. Seybold, G. Mezei, Are nanojars unique to copper? Solution and solid state characterization of high-symmetry octanuclear nickel(II)-pyrazolate complexes, Inorg. Chim. Acta 475 (2018) 65–72.
[11] V.W. Liyana Gunawardana, G. Mezei, Amplification of impurity upon complex formation: how a 2% ligand impurity lowers the corresponding complex purity to 50%, New J. Chem. 42 (2018) 17195–17202.
[12] a) W.A. Al Isawi, M. Zeller, G. Mezei, Capped nanojars: Synthesis, solution and solid-state characterization, and atmospheric CO_2 sequestration by selective binding of carbonate, Inorg. Chem. 60 (2021) 13479–13492;
b) W.A. Al Isawi, G. Mezei, Doubling the carbonate-binding capacity of nanojars by the formation of expanded nanojars, Molecules 26 (2021) 3083.
[13] W.A. Al Isawi, M. Zeller, G. Mezei, Tribenzyl(methyl)ammonium: a versatile counterion for the crystallization of nanojars with incarcerated selenite and phosphite ions and tethered pyrazole ligands, Cryst. Growth Des. 22 (2022) 1398–1411.
[14] M.M. Mitchell, V.W. Liyana Gunawardana, G. Ramakrishna, G. Mezei, Pyrene-functionalized fluorescent nanojars: synthesis, mass spectrometric, and photophysical studies, ACS Omega 6 (2021) 33180–33191.
[15] S.G. Kaler, ATP7A-related copper transport diseases – emerging concepts and future trends, Nat. Rev. Neurol 7 (2011) 15–29.
[16] Z. Tümer, L.B. Møller, Menkes disease, Eur. J. Hum. Genet 18 (2010) 511–518.
[17] A. Ala, A.P. Walker, K. Ashkan, J.S. Dooley, M.L. Schilsky, Wilson's disease, Lancet 369 (2007) 397–408.
[18] G. Crisponi, V.M. Nurchi, D. Fanni, C. Gerosa, S. Nemolato, G. Faa, Copper-related diseases: from chemistry to molecular pathology, Coord. Chem. Rev. 254 (2010) 876–889.
[19] G. Hao, Z.P. Xu, L. Li, Manipulating extracellular tumour pH: an effective target for cancer therapy, RSC Adv. 8 (2018) 22182–22192.
[20] V. Kumar, K. Kaur, G.K. Gupta, A.K. Sharma, Pyrazole containing natural products: synthetic preview and biological significance, Eur. J. Med. Chem. 69 (2013) 735–753.
[21] A. Ansari, M. Ali, Asif, Shamsuzzaman, Review: biologically active pyrazole derivatives, New J. Chem. 41 (2017) 16–41.
[22] T. Kosuge, H. Okeda, Nonylpyrazole, a new antimicrobial substance, J. Biochem. 41 (1954) 183–186.

[23] a) J. Brent, Fomepizole for ethylene glycol and methanol poisoning, New Engl. J. Med. 360 (2009) 2216–2223;
b) L.I. Velez, G. Shepherd, Y.C. Lee, D.C. Keyes, Ethylene glycol ingestion treated only with fomepizole, J. Med. Toxicol. 3 (2007) 125–128.
[24] E. Sletten, Crystallographic studies of metal-nucleotide base complexes. I. Triclinic bis-(6-aminopurine)copper(II) tetrahydrate, Acta Crystallogr.s Sect. B 25 (1969) 1480–1491.
[25] a) P. de Meester, A.C. Skapski, Crystal structure of dichlorotetra-μ-adenine-dicopper(II) chloride hexahydrate, J. Chem. Soc. A 2167–2169 (1971);
b) A. Terzis, A.L. Beauchamp, R. Rivest, Crystal and molecular structure of diaquotetra-μ-adeninediaquodicopper(I) perchlorate dihydrate, $[Cu_2(C_5H_5N_5)_4(H_2O)_2](ClO_4)4+2H_2O$, Inorg. Chem. 12 (1973) 1166–1170.
[26] a) B.J.M. Leite Ferreira, P. Brandão, A.M. Dos Santos, Z. Gai, C. Cruz, M.S. Reis, T. M. Santos, V. Félix, Heptacopper(II) and dicopper(II)-adenine complexes: synthesis, structural characterization, and magnetic properties, J. Coord. Chem. 68 (2015) 2770–2787;
b) J. Thomas-Gipson, R. Pérez-Aguirre, G. Beobide, O. Castillo, A. Luque, S. Pérez-Yáñez, P. Román, Unravelling the growth of supramolecular metal–organic frameworks based on metal-nucleobase entities, Cryst. Growth Des. 15 (2015) 975–983.
[27] J. Li, L. Jiang, S. Chen, A. Kirchon, B. Li, Y. Li, H.-C. Zhou, Metal–organic framework containing planar metal-binding sites: efficiently and cost-effectively enhancing the kinetic separation of C_2H_2/C_2H_4, J. Am. Chem. Soc. 141 (2019) 3807–3811.
[28] W. Henderson, J.S. McIndoe, Mass spectrometry of inorganic and organometallic compounds; John Wiley & Sons: Chichester, U.K., 2005, pp 117−119.